# Waveform cross correlation as a tool of mining explosion identification – the joint use of seismic array Mikhnevo and IMS array AKASG

Dmitry Bobrov[1], Ivan Kitov[2], Mikhail Rozhkov[1], and Irina Sanina[2] (1 - International Data Centre, CTBTO, 2 - Institute of Geosphere Dynamics, RAS)

CTBTO PREPARATORY COMMISSION | preparatory commission for the comprehensive nuclear-test-ban treaty organization

**Abstract.** There are hundreds of mines and quarries within the Russian platform using blasts with varying yields and firing schemes. Since the East-European platform is an aseismic zone mining-related explosion occupy a larger part of the seismic catalogue issued by the Geophysical Service of the Russian Academy of Sciences for this seismic region, with data chiefly provided by seismic array Mikhnevo (***MHVAR***, 54.950 N; 37.767 E). This array was deployed and operated by the Institute of Geospheres Dynamics (IDG) of the Russian Academy of Sciences in 2004. Mining explosions represent a major challenge for unbiased interpretation of natural seismicity in seismotectonic studies and for seismic monitoring under the Comprehensive Nuclear-Test-Ban Treaty (CTBT). Moreover, the task of finding and indentifying the nature of various seismic events in aseismic areas is more difficult because the size (magnitude, yield, energy) of studied events is small. Our main task is to evaluate the benefit of joint usage of (academic) seismic array Mikhnevo and seismic array AKASG of the International Monitoring System for the study of mining activity within the Russian platform. The advantage of location at regional distances from several major quarries and the availability of historical bulletins/ catalogues of mining explosions recorded by MHVAR allow estimating the increase in resolution and identification power of two arrays. Waveform data obtained by MHVAR and AKASG from quarries Mikhailovskiy, Stoylenskiy, and Lebedinskiy are processed jointly using waveform cross correlation technique in order to find similar signals. Since the latter two quarries are separated by a few kilometers, there exists a problem to accurately identify their seismic waves. We demonstrate that the cross correlation technique allows reducing the threshold of repeated events by an order of magnitude as well as accurately identifying mining explosions separate by several kilometers. The performance of cross correlation critically depends on the quality of waveform templates recorded from a carefully selected set of master events for each of the studied mines. We also test the possibility to use the Principal Component Analysis to produce sets of synthetic templates, which best fit the whole set of master events for a given mine.

## Conclusion

- IMS array stations can be helpful in improvement of the IDG catalogue of mining events
- Additional stations provide higher accuracy of location and origin times estimates
- Waveform cross correlation improves detection capability and effectively rejects wrong detections
- The analysis of mining activity within the Russian platform justifies the use of waveform cross correlation for automatic detection/association of repeated events
- Joint use of standard and cross correlation detection/association provide a prototype procedure for automatic recovery of aftershock sequence at the IDC

**Seismic Array MHVAR**
IDG runs MHVAR array since 2004

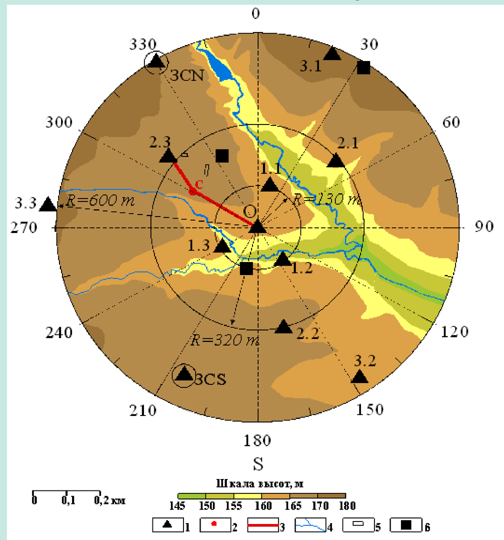

**Mining blasts measured at MHVAR**
IDG catalogue includes thousands of mining events

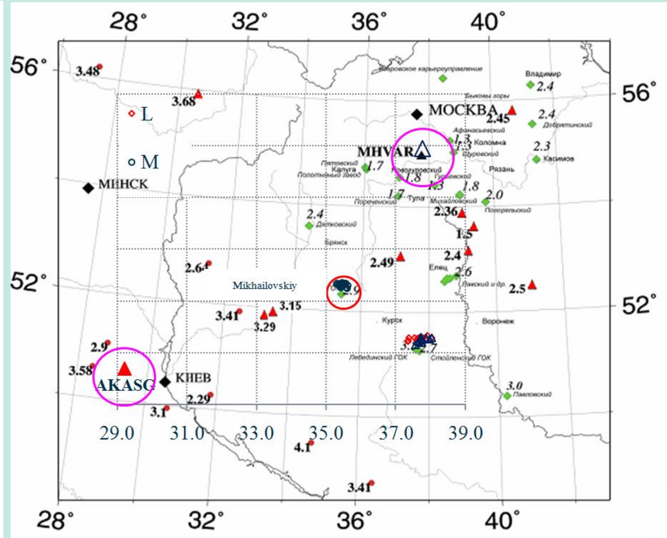


More than 50 areas at regional and near regional distances with different levels of mining activity have been identified by MHVAR. Since 2004, thousands of events have been reported in the IDG seismic catalogue as mining explosions. The IDG publishes this mining event catalogue as a part of the annual issues of "Earthquakes in Russia", which is available for the broader geophysical community.

The map shows several selected mines at near-regional distances where MHVAR successfully detects events with magnitudes 1.0 and lower.

We also show a few selected mines at regional distances with the largest events of magnitude (ML) 2.0 and above. Such events should be also detected by IMS arrays.

**Mikhailovskiy mine**
52.25 N -52.35 N 35.30 E – 35.61 E

Annual statistics at MHVAR

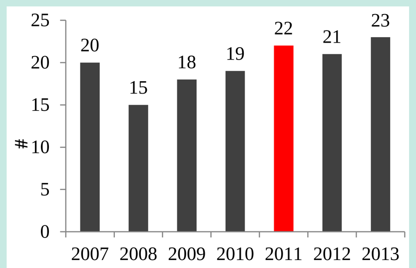


Magnitude distribution

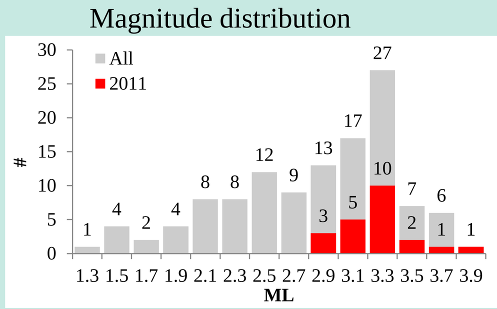


SM3-KV RESPONSE FUNCTION

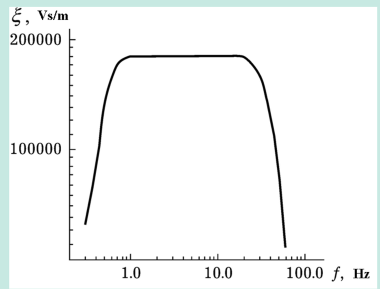


ARRAY RESPONSE FUNCTION

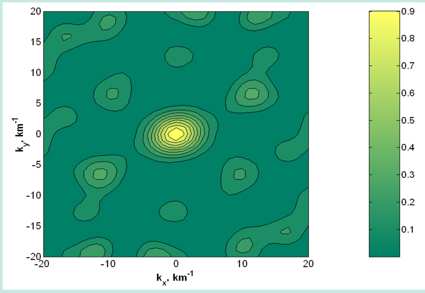

Typical regional waveforms

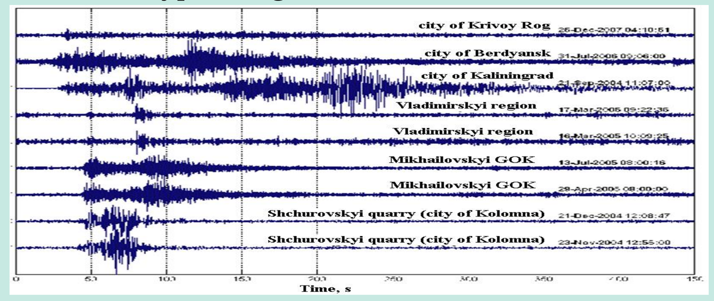


Joint interpretation of signals detected by MHVAR and IMS arrays allows significant improvements in signal detection, location, characterization and identification of events in the IDG catalogue when the historical data are revisited. The work on joint analysis of the IDG and IMS data is possible under the **"Contract for limited access to IMS data and IDC products"** between the CTBTO and IDG, which allows obtaining data through 2011. To begin with, we have chosen blasts with larger magnitudes from well-known ironstone mine Mikhailovskiy (red circle), which is situated at regional distances somewhere between MHVAR (~330 km) and IMS array AKASG (~470 km).

Figure above depicts a satellite image of the Mikhailovskiy quarry. This is a tremendous crater with the length of approximately 6 km. From this mine, MHVAR detects from 15 to 23 blasts per year. These blasts are usually conducted near round time at 8:00 and 9:00 UTC. Origin time is a good discrimination parameter for quarry blasts, but sometimes the blast time is shifted by minutes. Magnitudes of these events vary between 1.3 and 3.9.

Considering the lower accuracy of one station magnitude estimates we suggest that actual weights of explosive in the detected Mikhailovskiy blasts does not vary by 400 times, as the magnitude difference of 2.6 indicates. However, some variation in yield is possible. In 2011, MHVAR detected events identified as blasts at Mikhailovskiy mine. We focus on these events and first carry out signal detection from these events at AKASG.

In the current study of mining activity within the Russian platform, we use the advantages of location and historical bulletins/catalogues of mining explosions recorded by small-aperture seismic array Mikhnevo (MHVAR). The Institute of Geospheres Dynamics (IDG) of the Russian Academy of Sciences runs seismic array ***MHVAR*** (54.950N; 37.767E) since 2004. Small-aperture seismic array "Mikhnevo" includes ten vertical stations (solid triangles), with one station in the geometrical centre of the array (C00) and other nine stations distributed over three circles with radii of 130 m, 320 m, and 600 m. The array aperture in approximately 1.1 km. Two 3C stations (solid triangles in circles) were added to the outer circle in order to improve the overall stations sensitivity (detection threshold) and resolution. All stations are equipped with short-period seismometers SM3-KV, which are characterized by flat response between 0.8 Hz and 30 Hz and gain of 180,000 [Vs/m]. Later, a 3C broad band station (BB) was installed in the centre of the array for surface wave measurements. The array response function (only for 12 vertical channels) is similar to that for many small-aperture arrays. Such arrays are designed to measure high-frequency signals from regional and near-regional sources with magnitudes above 2.0.

**Principal Component Analysis MHVAR**

P-wave 13 waveforms | S-wave 8 + 7 waveforms | Rg-wave 12 waveforms

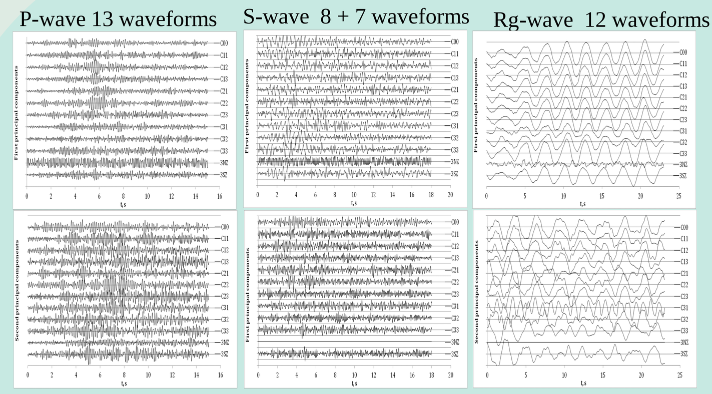

**Quality of CC detections: FK-analysis of CC-traces**

PCA_P1 | PCA_S1 | Actual P | Actual S

07/01
07/20
08/03

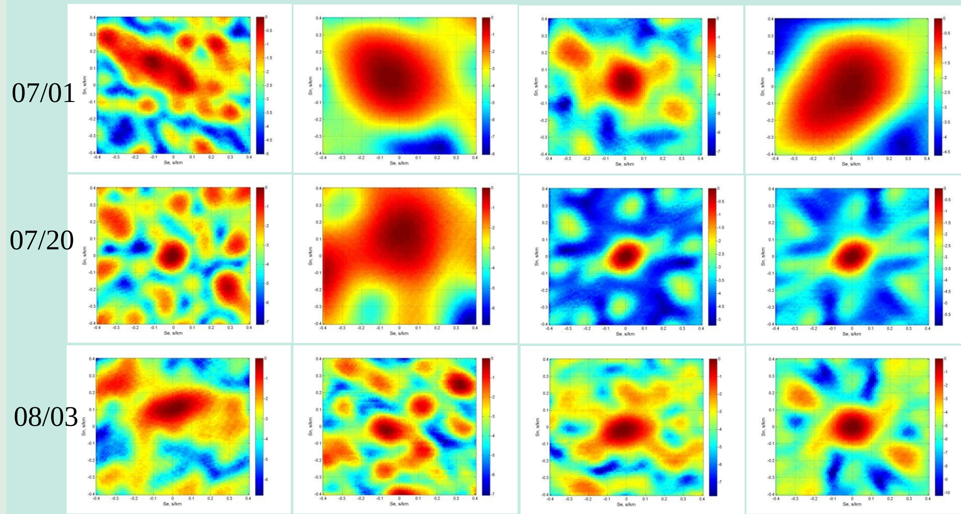

For cross correlation detections, there exists an efficient way to check detection quality – FK analysis applied to CC-traces. We present several examples for the PCA templates as well as for actual P- and S-wave templates. Specifically, we show FK for three days 07/01, 07/20, and 08/03. For a good detection, the peak of energy at FK-diagram should be in the centre since cross correlation between template (master) and sought (slave) signals are synchronized over all channels in spite of varying times of signal arrivals at these channels. The delay patter of the slave signal must accurately repeat the delay pattern of the master signal. These figures illustrate good performance of the selected templates. For a valid detection from Mikhailovskiy mine, we have introduced a constraint of 0.1 s/km for the deviation of peak FK from the centre. Detections with larger deviations are rejected.

**Performance of actual MHVAR waveforms and the PCA templates**

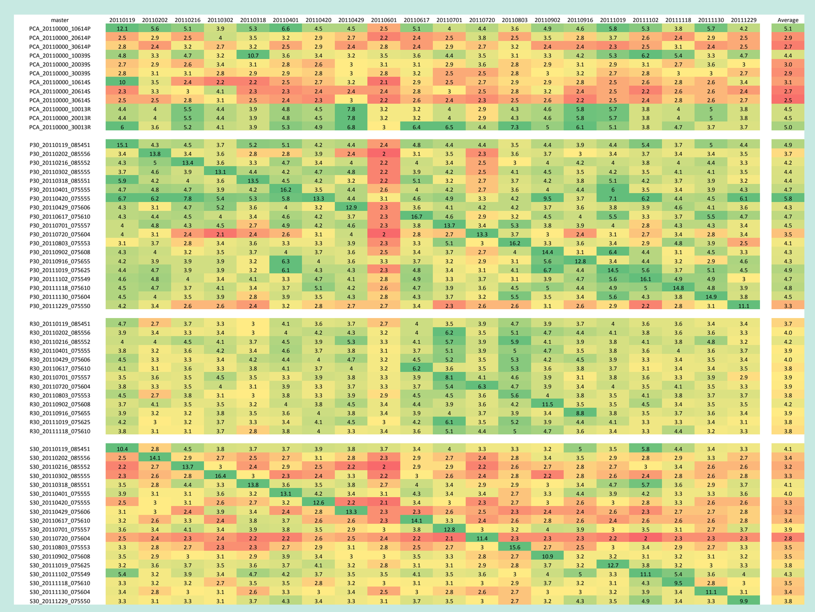

**P-wave first components**

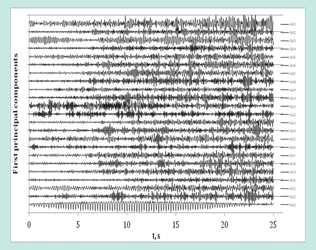


**PCA cross correlation with waveforms at individual channels**

| | S1 | S2 | S3 | S4 | S5 | S6 | S7 | S8 | S9 | S10 | S11 | S12 | S13 | S14 | S15 | S16 | S17 | S18 |
|---|---|---|---|---|---|---|---|---|---|---|---|---|---|---|---|---|---|---|
| AK1 | 0.88 | 0.88 | 0.28 | 0.44 | 0.24 | 0.28 | 0.08 | 0.15 | 0.24 | 0.31 | 0.16 | | 0.16 | 0.15 | 0.35 | 0.20 | 0.24 | 0.14 |
| AK2 | 0.92 | 0.92 | 0.38 | 0.09 | 0.22 | 0.14 | 0.23 | 0.15 | 0.19 | 0.15 | 0.10 | | 0.18 | 0.32 | 0.30 | 0.31 | 0.16 | 0.14 |
| AK3 | 0.80 | 0.80 | 0.25 | 0.18 | 0.34 | 0.07 | 0.40 | 0.13 | 0.27 | 0.25 | 0.18 | 0.52 | 0.18 | 0.23 | 0.32 | | | 0.11 |
| AK4 | 0.90 | 0.90 | 0.22 | 0.08 | 0.18 | | 0.44 | 0.19 | 0.17 | 0.20 | 0.13 | 0.16 | 0.19 | 0.34 | 0.09 | 0.24 | 0.20 | 0.13 |
| AK5 | 0.89 | 0.89 | 0.42 | 0.17 | 0.13 | 0.07 | 0.24 | 0.16 | 0.16 | 0.25 | 0.09 | 0.27 | 0.17 | 0.32 | 0.20 | 0.28 | 0.25 | 0.19 |
| AK6 | 0.96 | 0.96 | 0.20 | 0.14 | 0.32 | 0.11 | 0.25 | 0.13 | 0.15 | 0.21 | 0.17 | 0.30 | 0.18 | 0.24 | 0.21 | 0.19 | 0.15 | 0.17 |
| AK7 | 0.92 | 0.92 | 0.35 | 0.13 | 0.26 | 0.08 | 0.17 | 0.12 | 0.17 | 0.15 | 0.29 | 0.22 | 0.20 | 0.30 | 0.36 | 0.19 | 0.17 | 0.17 |
| AK8 | 0.94 | 0.94 | 0.13 | 0.15 | 0.30 | 0.09 | 0.32 | 0.10 | 0.17 | 0.11 | 0.25 | 0.28 | 0.29 | 0.22 | 0.21 | 0.20 | 0.17 | 0.15 |
| AK9 | 0.29 | 0.29 | 0.31 | 0.10 | -0.24 | 0.04 | 0.65 | | 0.07 | 0.68 | 0.06 | 0.05 | 0.04 | 0.06 | 0.04 | -0.05 | 0.07 | 0.10 |
| AK10 | 0.85 | 0.85 | 0.22 | 0.14 | 0.20 | 0.15 | 0.46 | 0.15 | 0.17 | 0.27 | 0.26 | 0.39 | 0.46 | 0.22 | 0.24 | 0.26 | 0.21 | 0.28 |
| AK11 | 0.98 | 0.98 | 0.29 | 0.08 | 0.17 | 0.13 | 0.21 | 0.21 | | | | | | | | | | 0.18 |
| AK12 | 0.99 | 0.99 | 0.25 | 0.15 | 0.20 | 0.16 | 0.21 | 0.09 | 0.14 | 0.09 | 0.14 | 0.13 | 0.13 | 0.13 | 0.12 | 0.15 | 0.16 | 0.22 |
| AK13 | 0.93 | 0.93 | 0.29 | 0.17 | 0.15 | 0.13 | 0.28 | 0.15 | 0.26 | 0.17 | 0.22 | 0.24 | 0.18 | 0.27 | 0.17 | 0.22 | 0.18 | 0.12 |
| AK14 | 0.92 | 0.92 | 0.29 | 0.16 | 0.18 | 0.12 | 0.36 | 0.15 | 0.18 | 0.28 | 0.14 | 0.18 | 0.08 | 0.20 | 0.29 | 0.40 | 0.18 | 0.20 |
| AK15 | 0.28 | 0.28 | 0.12 | 0.00 | 0.97 | 0.03 | 0.22 | 0.04 | 0.05 | 0.08 | 0.16 | 0.10 | -0.02 | 0.08 | -0.04 | 0.01 | 0.10 | 0.02 |
| AK16 | 0.19 | 0.19 | 0.00 | 0.02 | 1.00 | 0.02 | -0.04 | 0.03 | -0.05 | 0.05 | 0.03 | -0.03 | -0.06 | -0.09 | 0.07 | 0.07 | 0.02 | -0.06 |
| AK17 | 0.98 | 0.98 | 0.18 | 0.12 | 0.08 | 0.11 | 0.24 | 0.14 | 0.11 | 0.17 | | 0.25 | 0.19 | 0.18 | 0.28 | 0.19 | 0.22 | |
| AK18 | 0.54 | 0.54 | 0.61 | 0.14 | 0.37 | 0.10 | 0.25 | 0.04 | 0.42 | 0.23 | 0.46 | 0.37 | 0.25 | 0.22 | 0.21 | 0.32 | 0.23 | 0.10 |
| AK19 | 0.35 | 0.35 | 0.16 | 0.12 | 0.13 | 0.14 | 0.02 | -0.05 | 0.00 | 0.81 | 0.16 | 0.30 | 0.04 | 0.46 | 0.20 | 0.35 | 0.22 | 0.23 |
| AK20 | 0.28 | 0.28 | 0.03 | 0.05 | 0.14 | 0.14 | 0.02 | 0.01 | -0.01 | 0.39 | 0.02 | -0.01 | 0.09 | 0.23 | 0.11 | 0.95 | -0.05 | -0.06 |
| AK21 | 0.86 | 0.86 | 0.23 | 0.11 | 0.25 | 0.19 | 0.42 | 0.19 | 0.25 | 0.18 | 0.07 | 0.29 | 0.23 | 0.28 | 0.17 | 0.26 | 0.21 | 0.16 |
| AK22 | 0.38 | 0.38 | 0.11 | 0.16 | 0.05 | -0.04 | 0.66 | 0.13 | 0.40 | 0.04 | 0.24 | 0.40 | 0.62 | 0.27 | 0.39 | 0.04 | 0.19 | 0.13 |
| AK23 | 0.99 | 0.99 | 0.12 | 0.11 | 0.08 | 0.08 | 0.15 | 0.12 | 0.10 | 0.09 | 0.12 | | 0.11 | 0.12 | 0.19 | 0.09 | 0.12 | 0.08 |

For AKASG, the PCA does not provide any improvement on actual templates. This is because the loss of coherency between channels separated by several km for high-frequency waves. PCA components at individual channels are not synchronized as it works for MHVAR. Two tables illustrate low correlation between PCA components at a given channel with actual signals at this channel. Supposedly, all CCs should be above 0.5 since a good PCA has to contain the larger portion of all involved signals. For AKASG, one has to use more than 3 PCA components for effective detection.

**AKASG : selection of best templates 18 templates x 18 signals x 2 phases (P and S)**

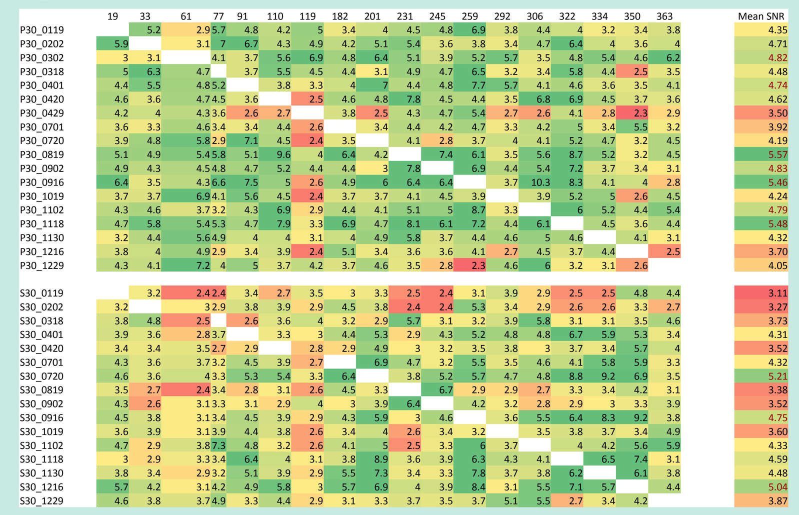

For AKASG, the PCA does not provide any improvement on actual templates. This is because the loss of coherency between channels separated by several km for high-frequency waves. PCA components at individual channels are not synchronized as it works for MHVAR. Two tables illustrate low correlation between PCA components at a given channel with actual signals at this channel. Supposedly, all CCs should be above 0.5 since a good PCA has to contain the larger portion of all involved signals. For AKASG, one has to use more than 3 PCA components for effective detection.

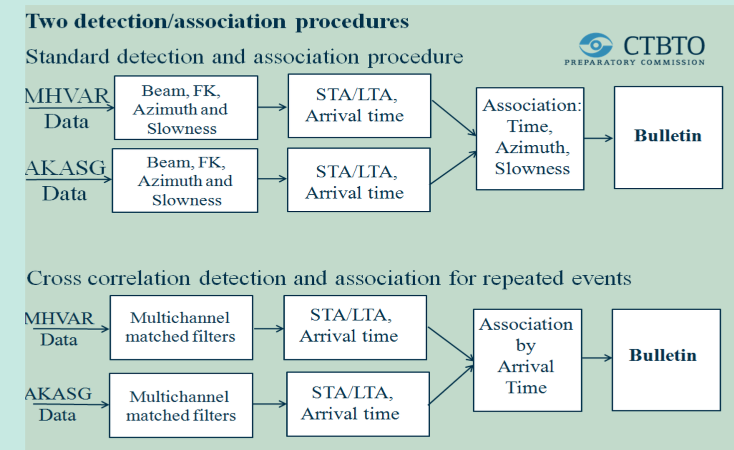


We have implemented to independent procedures for joint analysis of MHVAR and AKASG data. For standard detection procedure implemented at detection beams, we associate signals at two stations using arrival times (24 ± 5 s difference for P-wave), azimuth and slowness estimates. In preprocessing, all detections with azimuth and slowness out of predefined range are rejected. For cross correlation procedure, we use a few templates and detect signals at CC-channels with the same STA/LTA procedure. Association is based on arrival times only, since all irrelevant signals are eliminated by FK quality check. This procedure works well for areas with repeated events. When no template is available, the matched filter procedure is not possible. However, we will check if any of the IDG catalogue events is wrongly interpreted and associated with a different mine.

**MHVAR – typical waveforms from Mikhailovskiy**

P-waves | FK | S-waves | FK

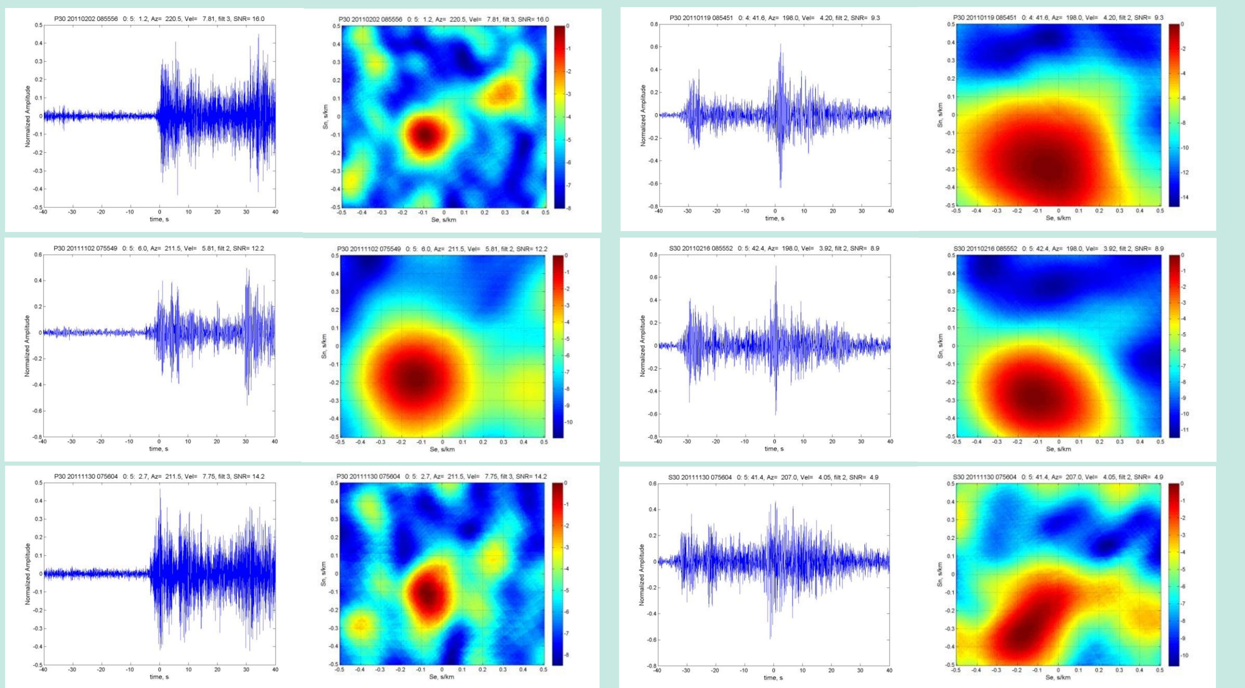

Typical waveforms from the Mikhailovskiy mine as detected at MHVAR. There are clear arrivals of P- and S-phases. We present beams obtained for the signals detected at all vertical channels available for given days. FK-analysis allows azimuth and slowness estimates, which can be also used for phase identification. For P-wave, velocity estimates vary between 5.8 km/s and 7.8 km/s. Azimuth to source is between 210 and 220 deg. Variations might be induced by effective loss of coherency in high-frequency signals from ripple-fired blasts. For S-waves, velocity estimates are close to 4.0 km/s, and azimuth varies near 200 deg.

Here we demonstrate the value added by IMS stations to the IDG catalogue. Under the "Contract for limited access to IMS data and IDC products" with the CTBTO, the IDG obtains an extensive data set from several IMS arrays at regional and far regional distances from the studied area. Signals from Mikhailovskiy mining events detected by MHVAR are sought at IMS arrays. Having arrival times at MHVAR and distances from the mine to MHVAR and IMS station AKASG we first processed continuous AKASG data to detect signals from known events.

**Waveforms from Mikhailovskiy: AKASG**

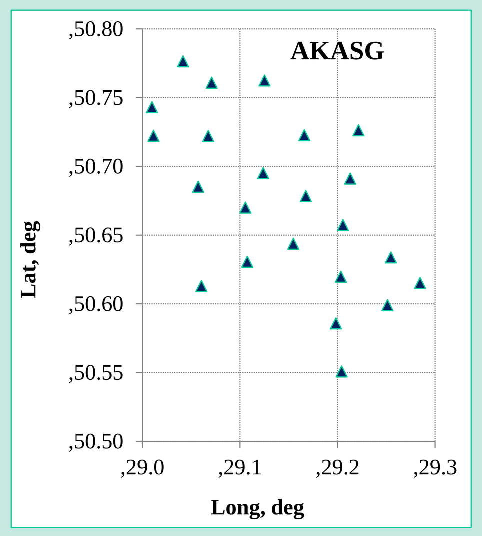


P-waves | S-waves

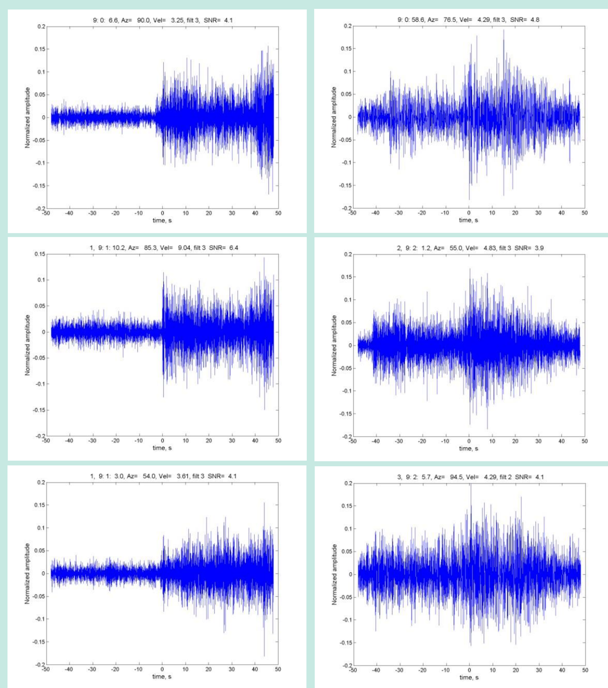

Station AKASG includes 23 vertical channels and has aperture of 25 km. All events were detected by standard STA/LTA procedure for those days where continuous data was available. We present several typical waveforms (detection beams) for P- and S-wave arrivals. Overall, these signals are similar to those at MHVAR and can be used for joint analysis – association of detections into events.

We present general statistics of detections and mining events in the IDG catalogue. Magnitude ML for Mikhailovskiy mine varies from 2.77 to 3.65 in 2011. Arrival times of automatic detections of P- and S-waves are refined by analysts. We also calculate automatic detections at AKASG and the time differences with the relevant MHVAR detections. Overall, these differences are around 24 s, in the range between 19 s and 27 s, but four events demonstrate smaller residuals of 17 s to 13 s. This might be the result of higher magnitudes measured in the seconds half of 2011 with automatic detection at AKASG finding earlier phases, which were under the ambient noise for the events in the first half. We refine this issue using cross correlation detector, which should reduce detection threshold.

**Cross correlation with waveforms from neighbouring mines**

Lebedinskiy 51.27 N 37.67 E; MHVAR distance ~410 km
Stoylenskiy 51.25 N 37.74 E; AKASG distance ~600 km


Discrimination between Lebedinskiy and Stoylenskiy mines is a challenge

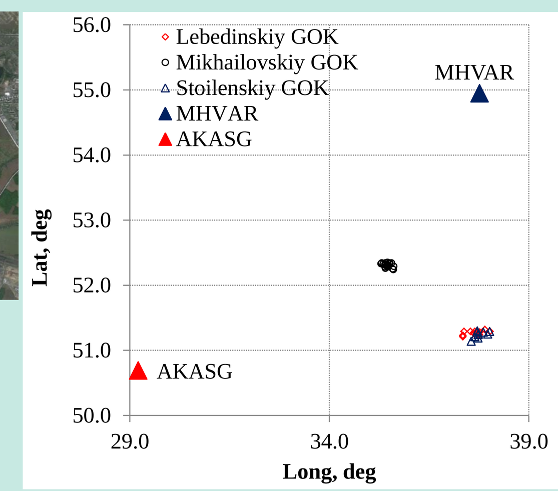


**Waveforms from Lebedinskiy and Stoylenskiy**

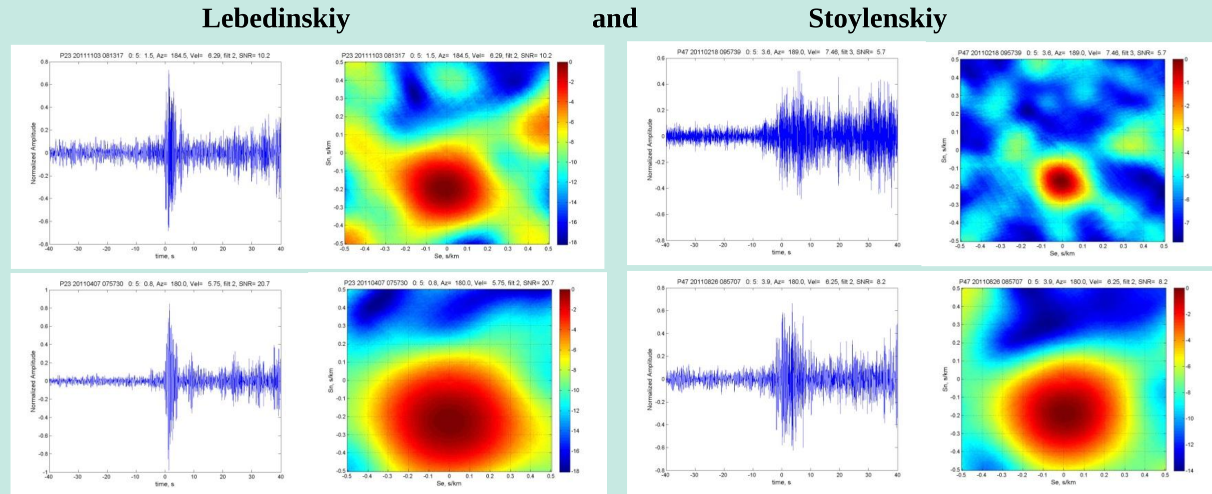

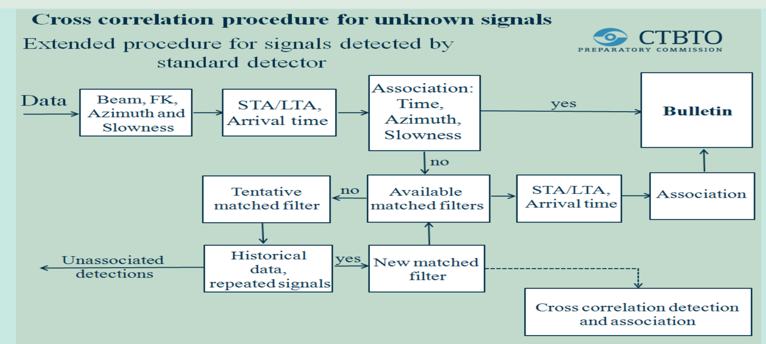


To start the cross correlation in a new place or add templates for new areas with repeated events we have developed a procedure. Standard detector provides new templates for retrospective processing and detection of similar signals in the past. After careful selection procedure and PCA analysis, the repeated signals are added to the set of templates. These templates are used in the standard detection in order to identify relevant phases for more accurate association of standard detections. The same templates start the independent matched filter procedure, which creates a bulletin of repeated events. The overall bulletin has to accommodate information both sets of events and provide accurate information on location, origin time, magnitude and type of events. For IDC purposes, this is a prototype procedure to automatically recover aftershock sequences.

**Separation and recovery of signals from different quarries arrived simultaneously enhance a CC-detector)**

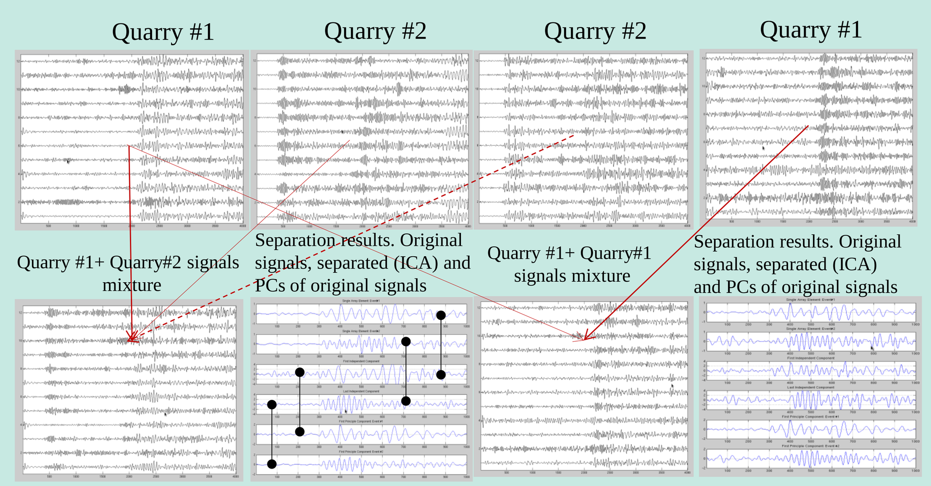


Solid lines indicate input waveforms for the actual example (mixture, and decomposition on the right). Dash line indicates typical waveform used to produce similar signal separation result. In first case primary phase of Q#1 event fall onto the secondary phase of Q#2 event making them visually inseparable. In second case all arrivals of both events fall on the same time producing visually a new event. A figure with separation results consists of: (1) a pair of input signals (from same channels) composing the mixture, (2) separated signals, and (3) first principle components of the array seismograms

We present the PCs to emphasize that the restored signals inherit the property of the whole array, not just some single component, since the best similarity is provided between the first PCs of the input array and the best Independent Component. The black vertical rounded lines indicate corresponding signals (omitted on right figure). Correlation coefficients between the original and restored signals are in a range (0.84, 0.92)

Preparatory Commission for the Comprehensive Nuclear-Test Ban Treaty Organization,
Provisional Technical Secretariat, Vienna International Centre, P.O. Box 1200, A-1400
Vienna, Austria. E-mail: Mikhail.Rozhkov@ctbto.org



IDG RAS
http://idg.chph.ras.ru/en

International Data Centre
http://www.ctbto.org